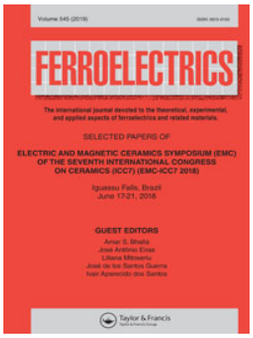

Ferroelectrics

ISSN: 0015-0193 (Print) 1563-5112 (Online) Journal homepage: https://www.tandfonline.com/loi/gfer20

# Production and characterization of (K Na)(Nb Cu)$O_3$ crystal fibers grown by micro-pulling-down method

M. V. S. Silva, A. M. E. Santo, S. L. Baldochi, A. M. Gonçalves, J. A. Eiras & M. H. Lente

**To cite this article:** M. V. S. Silva, A. M. E. Santo, S. L. Baldochi, A. M. Gonçalves, J. A. Eiras & M. H. Lente (2019) Production and characterization of (K Na)(Nb Cu)$O_3$ crystal fibers grown by micro-pulling-down method, Ferroelectrics, 545:1, 89-96, DOI: 10.1080/00150193.2019.1621693

**To link to this article:** https://doi.org/10.1080/00150193.2019.1621693

Published online: 22 Aug 2019.

FERROELECTRICS
2019, VOL. 545, 89–96
https://doi.org/10.1080/00150193.2019.1621693

Taylor & Francis
Taylor & Francis Group



# Production and characterization of (K Na)(Nb Cu)$O_3$ crystal fibers grown by micro-pulling-down method

M. V. S. Silva[a,b], A. M. E. Santo[a], S. L. Baldochi[c], A. M. Gonçalves[d], J. A. Eiras[d], and M. H. Lente[a]

[a]UNIFESP, ICT, São José dos Campos, SP, Brazil; [b]IFSP, São José dos Campos, SP, Brazil; [c]IPEN, São Paulo, SP, Brazil; [d]UFSCAR, DF, São Carlos, SP, Brazil

**ABSTRACT**

Cu-doped sodium potassium niobate single crystal fibers (KNN-Cu) were grown by the micro-pulling-down technique under different atmospheres, namely, argon, synthetic air and oxygen. The structural analysis revealed that all fibers were grown in the perovskite phase with no secondary phase. In comparison with the precursors powders, the results from EDX showed no significative chemical changes, suggesting that monocrystalline and stoichiometric KNN-Cu fibers were produced. The ferroelectric phase transitions characterized by thermal strain measurements corroborated this assumption. The dielectric results showed that the fibers produced under synthetic air presented the best results. Piezoresponse measurements revealed domains with typically orthorhombic symmetry morphology.

**ARTICLE HISTORY**
Received 17 June 2018
Accepted 1 April 2019

**KEYWORDS**
Ferroelectrics; sodium potassium niobate; single crystals; micro-pulling-down; PFM

## 1. Introduction

Ferroelectric materials have been investigated since the 1950s [1]. From the technological point of view, Pb-based ferroelectric materials such as Pb(Ti Zr)$O_3$ (PZT) and Pb(Mg Nb)$O_3$ (PMN) are the most commercialized compositions due to their wide applicability in piezoelectric transducers and actuators. However, the increase in the environment concerns and governmental restrictions have resulted in a strong demand for developing lead-free ferroelectric materials to replace PZT and PMN compositions [2, 3]. In this way, several lead-free ferroelectric compositions have been studied. Among them, $BaTiO_3$, (Na Bi)$TiO_3$ and (K Na)$NbO_3$ [2, 4, 5] are the most known compositions. Surely, (K Na)$NbO_3$ family (KNN) is one of the promising composition as Pb-free ferroelectric materials [5–7]. KNN presents a complex phase diagram such as PZT [8]. By appropriated Na/K ratio the piezoelectric and dielectric properties of KNN present higher values [6, 9] when compared to other lead-free ferroelectric oxides [10].

In comparison to ceramic counterparts, ferroelectric single crystals usually present superior piezoelectric properties, since the optimal crystallographic orientation can be achieved in crystals [11, 12]. However, up to 2000s almost all investigations on KNN were concentrated on ceramics. Nevertheless, over the last decade the interest in producing KNN in single crystal matrices has strongly raised [13–16]. Thus, several routes

CONTACT M. H. Lente mlente@unifesp.br
Color versions of one or more of the figures in the article can be found online at www.tandfonline.com/gfer.


**Figure 1.** Pictures of the as grown KNN-Cu fiber crystals growth in: a) Ar; b) $O_2$ and; c) synthetic air atmospheres. The fibers are on a millimeter paper.

have been employed, such as high temperature solution, micro-pulling-down, Czochralski and Bridgman techniques [17–20]. Among them, the micro-pulling-down technique ($\mu$-PD) is an attractive route due to its relative low cost. The growth of $KNbO_3$ single fiber crystal by $\mu$-PD method was firstly reported by Chani [21] and further by others [22, 23]. It was shown that the $\mu$-PD technique is a versatile method to grow high quality $KNbO_3$ crystals fibers. However, there is not too many reports viewing for improvements of physical properties of $KNbO_3$ crystals fibers through doping or compositional modification.

The present work aims to investigate the growth of Cu-doped $(KNa)NbO_3$ crystal fibers by the $\mu$-PD technique, starting from a stoichiometric powder composition and melted under different atmospheres. The ferroelectric domain morphology, structural, dielectric and thermomechanical properties were investigated.

## 2. Experimental

$(K_{0.48}Na_{0.52})$ $(Nb_{0.985}Cu_{0.015})O_3$ powders (KNN-Cu) were prepared by the conventional mixed-oxide process by using $K_2CO_3$ and $Na_2CO_3$ (Sigma-Aldrich, 99.0% purity), $Nb_2O_5$ (Sigma-Aldrich 99.9%) and CuO (Sigma-Aldrich, 99.5%). The carbonate powders were firstly dried in an oven for 3 h at 250 °C to eliminate adsorbed water. The precursors were weighted according to the desired stoichiometry and then mixed in a ball milling for 3 h in an ethanol solution. The dried material was calcined at 850 °C for 3.5 h.

KNN-Cu fiber crystals were obtained using the $\mu$-PD method with resistive heating. The doped crystals were grown under three different atmospheres: oxygen, argon, and synthetic air. The used crucibles were of platinum with size of $10 \times 6 \times 3$ mm, the capillary had external diameter of 1.2 mm with internal diameter of 1 mm. During growth, non-oriented KNN crystal was used as a seed. The seed crystal was brought into contact with the stoichiometric melt drop at 1232 °C (main heater) and the pulling down rate was 0.1 mm/min.

The structures of the KNN-Cu fibers were characterized at room temperature by X-ray diffraction (XRD) (Ultima IV, Rigaku) using $CuK_\alpha$. In order to make electrical measurements gold electrodes were sputtered on both faces of the fibers. Computer assisted dielectric characterizations were made employing an Impedance Analyzer HP 4194A from 1 kHz to 1 MHz at room temperature with a probing field of 500 mV. The thermal strain measurements were performed by using a NETZSCH 402 pushrod dilatometer. The measurements were performed at a cooling rate of 5 K/min with a

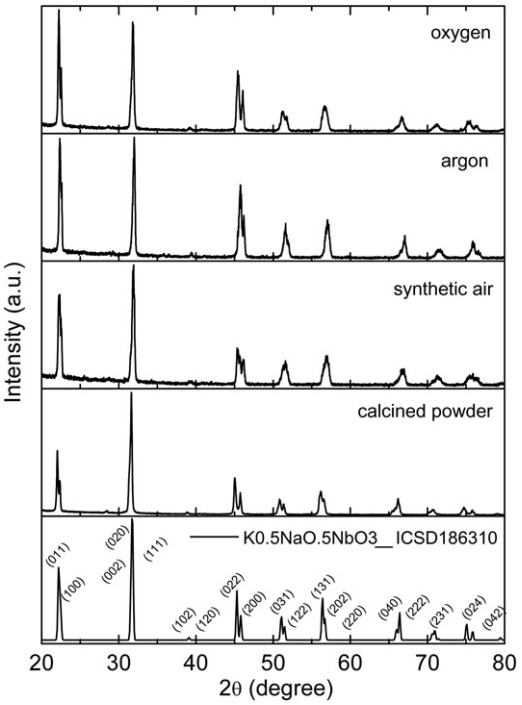


**Figure 2.** XRD patterns of the crushed crystal fibers. For the sake of comparison, the XRD patterns of the starting calcined powder is also shown.

constant force applied of 25 mN in He atmosphere in the temperature range from 550 °C to 50 °C. Thermal expansion technique (dilatometry) has been used successfully to investigate the nature of phase transitions in ferroelectric materials [24–26].

For the topography (AFM) and piezoresponse (PFM) analysis, a Shimadzu SPM9600 Atomic Force Microscope, adapted for piezoresponse measurements was utilized. Pt/Ir coated probes (PPP-EFM, from Nanosensors), with a force constant of 2.8 N/m, were utilized. The probing voltage and frequency were 4 $V_{pk}$ at 35 kHz, respectively. This frequency was empirically chosen, and it was far from any resonance. The images were obtained in the lateral part of the fibers.

## 3. Results and discussion

Figure 1a–c show the pictures of the KNN-Cu fiber crystals growth in Ar, $O_2$ and synthetic air atmospheres, respectively. The pictures reveal fibers with a good macroscopic homogeneity presenting a brownish color. The final diameters of the fibers were around 0.8 mm. This technique allowed us to grow fibers up to 10 mm long.

Figure 2 depict the XRD patterns obtained from the crushed crystal fibers. For the sake of comparison, the XRD patterns of the starting calcined powder are also shown. It is possible to note the formation of the perovskite structure with orthorhombic symmetry [27], thus maintaining the same symmetry of the precursor powder before the melting. In comparison to undoped KNN [3], the subtle shifty observed in our results

**Table 1.** EDS results from KNN-Cu crystal fibers prepared under different atmospheres.

| Elements | Synthetic air, nominal | Argon, nominal | Oxygen, nominal | Calculated |
|---|---|---|---|---|
| O | 28.14 | 28.68 | 28.69 | 28.03 |
| Na | 4.28 | 9.90 | 10.40 | 6.98 |
| K | 10.50 | 5.23 | 4.93 | 10.96 |
| Cu | 0.36 | 0.15 | 0.17 | 0.56 |
| Nb | 56.72 | 56.04 | 55.8 | 56.75 |

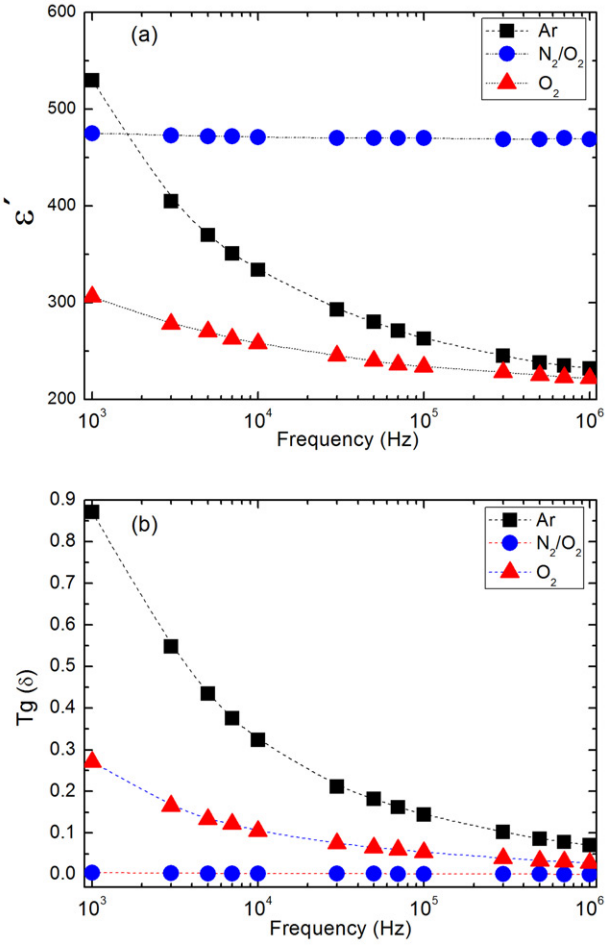


**Figure 3.** Frequency dependence of the relative dielectric permittivity ($\varepsilon'$) and the dielectric losses (tg$\delta$) of the KNN-Cu fibers measured at room temperature and growth under different atmospheres.

in the diffraction peaks in the KNN-Cu may be attributed to the substitution of $Nb^{+5}$ ions by the $Cu^{2+}$.

The EDS analyses of the crystals grown under the three different atmospheres are shown in Table 1. According to the results from EDS, the stoichiometry of the crystals is quite close to that of the calcined powder. Therefore, although the growth of the fibers does not occur in sealed crucible, this result reveals that the $\mu$-PD technique is able to pull stoichiometric KNN-Cu single crystal fibers.

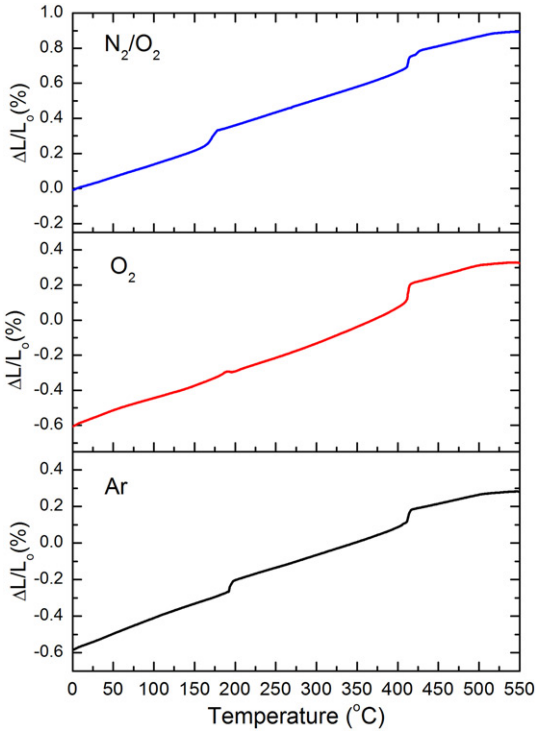


**Figure 4.** Thermal strain measurements of the KNN-Cu fibers growth under different atmospheres.

Figure 3a and b show, respectively, the frequency dependence of the relative dielectric permittivity ($\varepsilon$') and the dielectric losses (tg$\delta$) of the KNN-Cu fibers. The data reveal that the fiber grown in the synthetic air atmosphere ($N_2/O_2$) present the lowest dielectric loss and a higher and almost constant value for $\varepsilon$' (~475 at 1 kHz). The value for $\varepsilon$' is higher than those found for KNN-Cu ceramic counterparts [28–30]. In contrast, the fiber grown under Argon atmosphere present the highest tg($\delta$) with a strong frequency dispersion. This fact is credited to a higher formation of oxygen vacancies due to aggressive reducing atmosphere. The high values found for $\varepsilon$' at lower frequencies for the fiber grown under Argon atmosphere is due to undesirable contribution of the dielectric losses. However, the fiber that was grown under $O_2$ atmosphere also present a relative high dielectric loss. We expected values for tg($\delta$) similar or even lower than those observed in fibers grown under synthetic air. The reason for this apparent discrepancy is unknown and is still under investigation.

Figure 4a–c depict the thermal strain measurements performed in the KNN-Cu fibers. The data show that all fibers present two anomalies in the strain curve. One is at around 420 °C and another at around 210 °C. These anomalies can be associated to the paraelectric-ferroelectric and tetragonal-orthorhombic phases transitions, respectively. Indeed, these temperatures are in good agreement to those reported in the literature for ceramics with similar compositions [31, 32]. This fact corroborates our results from EDS analysis, that indicates that the crystal fibers are quite stoichiometry. Thus, such anomalies match the temperatures in which the respective phase transitions are expected.

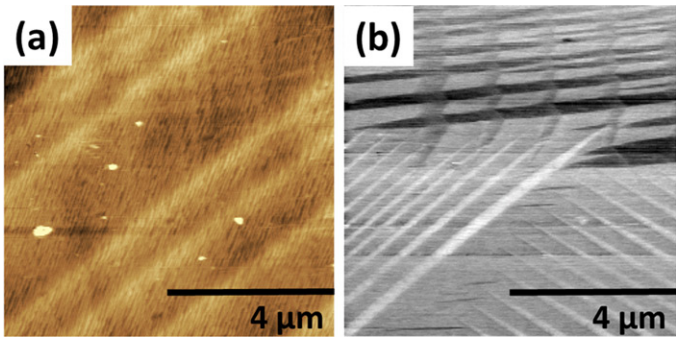


**Figure 5.** Topography and piezoresponse maps of the KNN-Cu fiber single crystals growth synthetic air.

Figure 5a–b show the topography and piezoresponse maps of the KNN-Cu single crystal growth under synthetic air. The images were obtained on the lateral surface of the fibers. A clear domain structure, typical for orthorhombic symmetry is observed [33]. This result corroborates the XRD data, in which an orthorhombic symmetry is verified. In addition, we can distinguish two different arrangements of domains. In the lower part of Figure 5d we observe two sets of domains, most likely separated by 90° walls, while the upper part is probably a composition of domains separated by 60° and 90° walls. Similar structures were observed in the parental phase $KNbO_3$ [32] and in $BaTiO_3$ orthorhombic single crystals [33]. It is interesting to point out that the domains form wedges, which were also observed by Wiesendanger [34]. A deeper investigation of the domain structures in the KNN + Cu fibers is reserved for a future work.

## 4. Conclusions

Stoichiometric Cu-doped sodium potassium niobate single crystal fibers were successfully grown under argon, synthetic air and oxygen atmospheres by the micro-pulling-down technique. The as grown fibers presented perovskite structure with absence secondary phase. The paraelectric-ferroelectric and tetragonal-orthorhombic phases transitions were characterized by thermal strain measurements. The dielectric results showed that the fibers produced under synthetic air present the better dielectric results, while the piezoresponse measurements revealed ferroelectric domains with morphology typical of orthorhombic symmetry.

## Acknowledgments

The authors thank Fundação de Amparo à Pesquisa do Estado de São Paulo (FAPESP), CNPq (Grant 163761/2017-5) and FINEP for financial support. The authors also thank Federal University of São Paulo for providing the core research facilities - NAPCEM.

## References

[1] B. Jaffe, W. R. Cook, and H. Jaffe, *Piezoelectric Ceramics* (Academic Press, London, UK, 1971).

[2] Y. Saito *et al.*, Lead-free piezoceramics, *Nature*. **432** (7013), 84 (2004). DOI: 10.1038/nature03028.

[3] L. Wu *et al.*, Influence of compositional ratio K/Na on physical properties in $(K_xNa_{1-x})NbO_3$ ceramics, *J. Appl. Phys*. **103** (8), 084116 (2008). DOI: 10.1063/1.2907866.

[4] J. Rodel *et al.*, Perspective on the development of lead-free piezoceramics, *J. Am. Ceram. Soc*. **89**, 1153 (2009). DOI: 10.1111/j.1551-2916.2009.03061.x.

[5] T. R. Shrout, and S. J. Zhang, Lead-free piezoelectric ceramics: alternatives for PZT? *J. Electroceram*. **19**, 111 (2007).

[6] L. Egerton and D. M. Dillon, Piezoelectric and dielectric properties of ceramics in the system potassium-sodium niobate, *J. Am. Ceram. Soc*. **42** (9), 438 (1959). DOI: 10.1111/j.1151-2916.1959.tb12971.x.

[7] P. Bomlai *et al.*, Effect of calcination conditions and excess alkali carbonate on the phase formation and particle morphology of $Na_{0.5}K_{0.5}NbO_3$ powders, *J. Am. Ceram. Soc*. **90** (5), 1650 (2007). DOI: 10.1111/j.1551-2916.2007.01629.x.

[8] D. W. Baker *et al.*, A comprehensive study of the phase diagram of $K_xNa_{1-x}NbO_3$, *Appl. Phys. Lett*. **95** (9), 091903 (2009). DOI: 10.1063/1.3212861.

[9] A. Hussain *et al.*, Dielectric, ferroelectric and field-induced strain behavior of $K_{0.5}Na_{0.5}NbO_3$-modified $Bi_{0.5}(Na_{0.78}K_{0.22})$TiO3 lead-free ceramics, *Ceram. Int*. **38** (5), 4143 (2012). DOI: 10.1016/j.ceramint.2012.01.074.

[10] P. K. Panda, Review: environmental friendly lead-free piezoelectric materials, *J. Mater. Sci*. **44** (19), 5049 (2009). DOI: 10.1007/s10853-009-3643-0.

[11] K. Harada *et al.*, Growth of Pb[(Zn1/3Nb2/3)0.91Tio.09]03 single crystal of ultrasonic transducer for medical application, *J. Intelligent Mater. Syst. Struct*. **10** (6), 493 (1999). DOI: 10.1106/UQ35-HFYR-PCX9-BPJL.

[12] *Handbook of Advanced Dielectric, Piezoelectric and Ferroelectric Materials*, Edited by Zuo-Guang Ye (CRC Press, Boston, MA, 2008).

[13] R. Saravanan *et al.*, Crystal growth and dielectric property of $Na_{0.5}K_{0.5}NbO_3$ and Mn-doped $Na_{0.5}K_{0.5}NbO_3$ single crystal grown by flux method, *Int. J. App. Phys. Mathem*. **2**, 208 (2012). DOI: 10.7763/IJAPM.2012.V2.91.

[14] S. Wada *et al.*, Enhanced piezoelectric properties of potassium niobate single crystals by domain engineering, *Jpn. J. Appl. Phys*. **43** (9B), 6692 (2004). DOI: 10.1143/JJAP.43.6692.

[15] S. A. Sheets *et al.*, Relaxor single crystals in the $(Bi_{1/2}Na_{1/2})1$-*x*Ba*x*Zr*y*$Ti_{1-y}O_3$ system exhibiting high electrostrictive strain, *J. Appl. Phys*. **90** (10), 5287 (2001). DOI: 10.1063/1.1410325.

[16] K. Chen *et al.*, Dielectric and piezoelectric properties of lead-free $0.95(K_{0.5}Na_{0.5})NbO_3$-$0.05LiNbO_3$ crystals grown by the Bridgman method, *J. Appl. Phys*. **101** (4), 044103 (2007). DOI: 10.1063/1.2562464.

[17] S. E. Park *et al.*, Nonstoichiometry and the long-range cation ordering in crystals of $(Na_{1/2}Bi_{1/2})TiO_3$, *J. Am. Ceram. Soc*. **77** (10), 2641 (1994). DOI: 10.1111/j.1151-2916.1994.tb04655.x.

[18] S. E. Park, S. J. Chung, and I. T. Kim, Ferroic phase transitions in (Na1/2Bi1/2)TiO3 crystals, *J. Am. Ceram. Soci*. **79** (5), 1290 (1996). DOI: 10.1111/j.1151-2916.1996.tb08586.x.

[19] Y. Hosono, K. Harada, and Y. Yamashita, Crystal growth and electrical properties of lead-free piezoelectric material $(Na_{1/2}Bi_{1/2})TiO_3$-$BaTiO_3$, *Jpn. J. Appl. Phys*. **40** (Part 1, No. 9B), 5722 (2001). DOI: 10.1143/JJAP.40.5722.

[20] T. V. Kruzina, V. M. Duda, and J. Suchanicz, Peculiarities of optical behavior of $Na_{0.5}Bi_{0.5}TiO_3$ single crystals, *J. Mater. Sci. Eng*. **87** (1), 48 (2001). DOI: 10.1016/S0921-5107(01)00689-4.

[21] V. I. Chani, K. Shimamura, and T. Fukuda, Flux growth of $KNbO_3$ crystals by pulling-down method, *Cryst. Res. Technol*. **34** (4), 519 (1999). DOI: 10.1002/(SICI)1521-4079(199904)34:4<519::AID-CRAT519>3.0.CO;2-A.

[22] R. Komatsu *et al.*, $KNbO_3$ plate crystal grown by micro-pulling-down method from stoichiometric melt, *J. Crystal Growth*. **401**, 772 (2014). DOI: 10.1016/j.jcrysgro.2013.12.071.

[23] R. Komatsu, Y. Okuma, H. Itoh, and Y. Akishige, Growth and characterization of potassium niobate fiber crystal from liquid with stoichiometric composition by $\mu$-PD method, *Electron. Comm. Jpn.* . **95**, 1126 (2012). DOI: 10.1002/ecj.10411.

[24] E. C. Subbarao, Studies on lead titanate ceramics containing niobium or tantalum, *J. Am. Ceram. Soc.* **43** (3), 119 (1960). DOI: 10.1111/j.1151-2916.1960.tb14324.x.

[25] T. Y. Tien, and W. G. Carlson, Effect of additives on properties of lead titanate, *J. Am. Ceram. Soc.* **45** (12), 567 (1962). DOI: 10.1111/j.1151-2916.1962.tb11060.x.

[26] B. Malic *et al.*, Linear thermal expansion of lead-free piezoelectric $K_{0.5}Na_{0.5}NbO_3$ ceramics in a wide temperature range, *J. Am. Ceram. Soc.* **94**, 2273 (2011). DOI: 10.1111/j.1551-2916.2011.04628.x.

[27] J. Tellier *et al.*, Extremely temperature-stable piezoeletric properties of ortorrombic phase in (K, Na)$NbO_3$ – based ceramics, *Solid State Sci.* **11** (2), 320 (2009). DOI: 10.1016/j.solidstatesciences.2008.07.011.

[28] S. Zhang *et al.*, Characterization of hard piezoelectric lead-free ceramics, *IEEE Trans. Ultrason. Ferroelectr. Freq. Control.* **56** (8), 1523 (2009). DOI: 10.1109/TUFFC.2009.1215.

[29] F. Azough *et al.*, Microstructure and piezoelectric properties of CuO added (K, Na, Li)$NbO_3$ lead-free piezoelectric ceramics, *J. Eur. Ceram. Soc.* **31** (4), 569 (2011). DOI: 10.1016/j.jeurceramsoc.2010.10.033.

[30] H.-Y. Park *et al.*, Effect of CuO on the sintering temperature and piezoelectric properties of $(Na_{0.5}K_{0.5})NbO_3$ lead-free piezoelectric ceramics, *J. Am. Ceram. Soc.* **91** (7), 2374 (2008). DOI: 10.1111/j.1551-2916.2008.02408.x.

[31] E. M. Alkoy, and M. Papila, Microstructural features and electrical properties of copper oxide added potassium sodium niobate ceramics, *Ceram. Int.* **36** (6), 1921 (2010). DOI: 10.1016/j.ceramint.2010.03.018.

[32] H. S. Han *et al.*, Hardening behavior and highly enhanced mechanical quality factor in$(K_{0.5}Na_{0.5})NbO_3$-based ceramics, *J. Eur. Ceram. Soc.* **37** (5), 2083 (2017).

[33] T. Limboeck and E. Soergel, Evolution of ferroelectric domain patterns in $BaTiO_3$ at the orthorhombic ↔ tetragonal phase transition, *Appl. Phys. Lett.* **105** (15), 152901 (2014).

[34] E. Wiesendanger, Domain structures in orthorhombic $KNbO_3$ and characterisation of single domain crystals, *Czech. J. Phys.* **23** (1), 91 (1973). DOI: 10.1007/BF01596882.